

A Theoretical Study of Addition of Organomagnesium Reagents to Chiral α -Alkoxy Carbonyl Compounds

Vicent S. Safont,* Vicente Moliner, Mónica Oliva, Raquel Castillo, Juan Andrés, Florenci González,[†] and Miguel Carda[†]

Departament de Ciències Experimentals and Departament de Química Inorgànica i Orgànica, Universitat Jaume I, Box 242, 12080 Castelló, Spain

Received December 12, 1995[⊗]

A theoretical study on the addition of organomagnesium reagents (CH_3Mg^+ , CH_3MgCl , $2\text{CH}_3\text{MgCl}$) to the carbonyl group of chiral α -alkoxy carbonyl compounds (2-hydroxypropanal, 3-hydroxybutanone, and 3,4-di-*O*-methyl-1-*O*-(trimethylsilyl)-*L*-erythrose) has been carried out. Analytical gradients SCF MO and second derivatives at the PM3 semiempirical procedure and the *ab initio* method at the HF/3-21G basis set level have been applied to identify the stationary points on potential energy surfaces. The geometry, harmonic vibrational frequencies, transition vector, and electronic structure of the transition structures have been obtained. The dependence of the results obtained upon the computing method and the model system is analyzed, discussed, and compared with available experimental data. The first step corresponds to the exothermic formation of a chelate complex without energy barrier. This stationary point corresponds to a puckered five-membered ring, determining the stereochemistry of the global process, which is retained throughout the reaction pathway. The second and rate-limiting step is associated to the C–C bond formation via 1,3-migration of the nucleophilic methyl group from the organomagnesium compound to the carbonyl carbon. For an intramolecular mechanism (addition of CH_3Mg^+ and CH_3MgCl to different carbonyl compounds) the transition structure can be described as a four-membered ring. The inclusion of a second equivalent of CH_3MgCl , corresponding to an intermolecular mechanism, decreases the barrier height, and the process can be considered as an assisted intermolecular mechanism: the first equivalent forms the chelate structure and the second CH_3MgCl carries out the nucleophilic addition to the carbonyl group. The most favorable pathway corresponds to an intermolecular mechanism via an anti attack. The analysis of the results reveals that the nature of transition structures for the intramolecular and intermolecular mechanisms is a rather robust entity. There is a minimal molecular model with a transition structure which describes the essentials of the chemical addition process, and the corresponding transition vector is an invariant feature.

Introduction

Due to their unusual value as reagents for general laboratory synthetic purposes, several studies have been reported for Grignard compounds.^{1–7} Development of enantioselective synthesis has revolutionized the organic chemist's ability to prepare compounds in enantiopure form. In particular, Grignard-type addition and reduction of chiral carbonyl compounds is one of the most extensively used reactions in synthetic organic chemistry, avoiding formation of undesirable diastereomers.^{8–10}

Although different theories based on coulombic, electronic, or orbital considerations have been proposed,^{8,9,11,12}

the origin of stereoselectivity remains uncertain due to the large number of different factors involved.^{8,10,13} Two models have been widely employed to predict the outcome of nucleophilic additions: (i) the seminal work of Cram,^{14,15} based on the substrate's bidentate ligation to the metal counteraction, chelation model,^{8,10,16–20} and (ii) the Felkin–Anh model,^{11,21,22} based mainly on steric and/or stereoelectronic arguments. However, the understanding of nucleophilic addition to carbonyl compounds is still a much debated area.^{23–31} On the basis of the stereochemical considerations, intermediate chelates were proposed

[†] Departament de Química Inorgànica i Orgànica.

[⊗] Abstract published in *Advance ACS Abstracts*, May 1, 1996.

(1) Baskin, C. P.; Bender, C. F.; Lucchese, R. R.; Bauschlicher, C. W.; Schaefer, H. F. *J. Mol. Struct.* **1976**, *32*, 125–131.

(2) Sakai, S.; Jordan, K. D. *J. Am. Chem. Soc.* **1982**, *104*, 4019–4021.

(3) Jasien, P. G.; Dykstra, C. E. *J. Am. Chem. Soc.* **1983**, *105*, 2089–2090.

(4) Jasien, P. G.; Dykstra, C. E. *J. Am. Chem. Soc.* **1985**, *107*, 1891–1895.

(5) Davis, S. R. *J. Am. Chem. Soc.* **1991**, *113*, 4145–4150.

(6) Smirnov, V. V.; Tyurina, L. A. *Russ. Chem. Rev. (Engl. Transl.)* **1994**, *63*, 55.

(7) Nemukhin, A. V.; Topol, I. A.; Weinhold, F. *Inorg. Chem.* **1995**, *34*, 2980–2983.

(8) Reetz, M. T. *Angew. Chem., Int. Ed. Engl.* **1984**, *23*, 556–569.

(9) Chen, X.; Hortelano, E. R.; Eliel, E. L.; Frye, S. V. *J. Am. Chem. Soc.* **1992**, *114*, 1778–1784.

(10) Reetz, M. T. *Acc. Chem. Res.* **1993**, *26*, 462–468.

(11) Anh, N. T. *Top. Curr. Chem.* **1980**, *88*, 145.

(12) Mead, K.; Macdonald, T. L. *J. Org. Chem.* **1985**, *50*, 422.

(13) Reetz, M. T.; Stanchev, S.; Haning, H. *Tetrahedron* **1992**, *48*, 6813.

(14) Cram, D. J.; Abd Elhafez, F. A. *J. Am. Chem. Soc.* **1952**, *74*, 3210.

(15) Cram, D. J.; Kopecky, K. R. *J. Am. Chem. Soc.* **1959**, *81*, 2748.

(16) Still, W. C.; MacDonald, J. H., III. *Tetrahedron Lett.* **1980**, *21*, 1031.

(17) Still, W. C.; Schneider, J. A. *Tetrahedron Lett.* **1980**, *21*, 1035.

(18) Eliel, E. L. *Asymmetric Synthesis*; Academic: New York, 1983; Vol. 2, Part A, p 125.

(19) Eliel, E. L.; Frye, S. V.; Hortelano, E. R.; Chen, X.; Bai, X. *Pure Appl. Chem.* **1991**, *63*, 1591.

(20) Huryn, D. M. *Comprehensive Organic Synthesis*; Pergamon: Oxford, U.K., 1991; Vol. 1, p 49.

(21) Chérest, M.; Felkin, H.; Prudent, N. *Tetrahedron Lett.* **1968**, *2199*.

(22) Anh, N. T.; Eisenstein, O. *Nouv. J. Chem.* **1977**, *1*, 161.

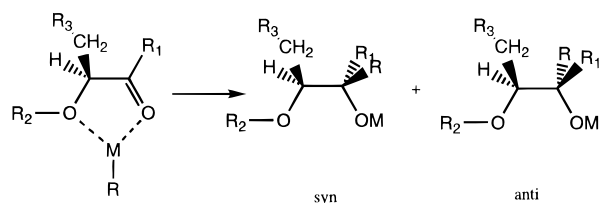
(23) Metha, G.; Khan, F. A. *J. Am. Chem. Soc.* **1990**, *112*, 6140.

(24) Wong, S. S.; Paddon-Row, M. N. *J. Chem. Soc., Chem Commun.* **1991**, 327–330.

(25) Frenking, G.; Köhler, K. F.; Reetz, M. T. *Angew. Chem., Int. Ed. Engl.* **1991**, *30*, 1146.

(26) Wu, Y.; Houk, K. N.; Florez, J.; Trost, B. M. *J. Org. Chem.* **1991**, *56*, 3656.

Scheme 1. Schematic Representation for the Chelate-Controlled Addition of an Organometallic Reagent (M-R) to the Carbonyl Group of a Chiral α -Alkoxy Carbonyl Compound^a



^a Two diastereoisomers with different orientation of R with respect to CH_2R_3 can be obtained. The syn diastereoisomer is obtained when the nucleophilic attack of R takes place on the same face of the plane, defined by the carbonyl group and the α -carbon atom, where CH_2R_3 is located in the chelate complex.

which were thought to react selectively from the sterically less hindered π face. In the case of chiral α -alkoxy ketones, the formation of diastereoisomers with anti conformation is consistently favored¹⁵ (Scheme 1). Several theoretical works addressed this issue;^{24,32–36} however, no conclusive interpretation has been obtained.^{8,13}

Currently, quantum mechanical calculations are recognized as a useful tool in research related to elucidation of molecular reaction mechanisms.^{37,38} The understanding at the molecular level of a reaction mechanism for a given chemical reaction requires a detailed knowledge of stationary points: reactants, transition structure (TS), products, and possible intermediates on the potential energy surface (PES). In particular, theoretical characterization of TSs provides a source of information, independent from experimental studies, concerning the geometry, electronic structure, and stereochemistry along the reaction pathway.³⁹

Recently, we have carried out a diastereoselective synthesis of enantiomeric tertiary alcohols via nucleophilic additions to L-erythulose derivatives^{40,41} with considerable utility in the synthesis of several oxygenated chiral natural products like carbohydrates, macrolide antibiotics, and antitumor ansamycins.^{42–44} Despite the synthetic progress in the addition of C-nucleophiles such

as Grignard reagents to chiral α -alkoxy carbonyl compounds, fundamental questions on molecular reaction mechanism still remain because the experimental data are always based only on the diastereomeric product ratio. Neither our previous experimental work^{40,41} nor related calculations^{10,32–35,45,46} offer a conclusive solution in understanding the mechanistic basis for these stereoselective reactions.

In conjunction with our interest in exploring new possibilities in asymmetric synthesis, we describe herein a theoretical study of the possible reaction pathways associated with the addition of different organomagnesium reagents to the carbonyl group of different models representing chiral α -alkoxy carbonyl compounds. The intention is to illustrate the important interplay between experimental and theoretical efforts in the elucidation of such reactions, showing how theory may contribute significantly to the unravelling of reaction mechanisms in cases which are experimentally unfeasible or at least very unattractive.

Methods and Models

A complete application of the *ab initio* method is generally prohibitive in terms of computational effort for any but the smallest systems. Furthermore, semiempirical procedures are intended for studying large molecular systems of organic chemical interest. Semiempirical methods have progressed over the past few years to a surprising level of accuracy and reliability, considering the limitations of the underlying approximations.^{47,48} Semiempirical calculations have been made by using the PM3⁴⁹ method, and *ab initio* calculations were made at the HF/3-21G⁵⁰ level. The calculations have been performed with the GAUSSIAN92/DFT program.⁵¹

The Berny analytical gradient optimization routines^{52,53} were used for optimization. The requested convergence on the density matrix was 10^{-9} atomic units, and the threshold value of maximum displacement was 0.0018 Å and that of maximum force was 0.000 45 hartree/bohr. The nature of each stationary point was established by calculating and diagonalizing the Hessian matrix (force constant matrix). An eigenvalue following algorithm⁵⁴ was used for locating the TSs, which were characterized by means of a normal mode analysis, and the unique imaginary frequency associated with transition vector (TV)⁵⁵ has been characterized. The nature of all TSs was verified by tracing the intrinsic reaction coordinate (IRC)⁵⁶ from the TS to the two lower energy structures it connects by using the second-order González-Schlegel integration method.^{57,58}

The control space, dominant components of TV, includes all degrees of freedom defining the bond forming/breaking process and is reported for the calculated TSs. In the terminology used

(27) Wu, Y.; Tucker, J. A.; Houk, K. N. *J. Am. Chem. Soc.* **1991**, *113*, 5018.

(28) Hahn, J. M.; le Noble, W. J. *J. Am. Chem. Soc.* **1992**, *114*, 1916.

(29) Kumar, V. A.; Venkatesan, K.; Ganguly, B.; Chandrasekhar, J.; Khan, F. A.; Metha, G. *Tetrahedron Lett.* **1992**, *33*, 2069.

(30) Li, H.; le Noble, W. J. *Recl. Trav. Chim. Pays-Bas* **1992**, *111*, 199.

(31) Wu, Y.-D.; Houk, N. K.; Paddon-Row, M. N. *Angew. Chem.* **1992**, *104*, 1087.

(32) Frenking, G.; Köhler, K. F.; Reetz, M. T. *Tetrahedron* **1991**, *47*, 9005–9018.

(33) Frenking, G.; Köhler, K. F.; Reetz, M. T. *Tetrahedron* **1993**, *49*, 3983–3994.

(34) Frenking, G.; Köhler, K. F.; Reetz, M. T. *Tetrahedron* **1993**, *49*, 3971–3982.

(35) Mori, S.; Nakamura, M.; Nakamura, E.; Koga, N.; Morokuma, K. *J. Am. Chem. Soc.* **1995**, *117*, 5055–5065.

(36) Coxon, J. M.; Kouk, K. N.; Luijbrand, R. T. *J. Org. Chem.* **1995**, *60*, 418–427.

(37) Williams, I. H. *Chem. Soc. Rev.* **1993**, 277.

(38) Skancke, P. N. *Acta Chem. Scand.* **1993**, *47*, 629–648.

(39) Stewart, J. D.; Liotta, L. J.; Benkovic, S. J. *Acc. Chem. Res.* **1993**, *26*, 396.

(40) Carda, M.; González, F.; Rodríguez, S.; Marco, J. A. *Tetrahedron: Asymmetry* **1992**, *3*, 1511–1514.

(41) Carda, M.; González, F.; Rodríguez, S.; Marco, J. A. *Tetrahedron: Asymmetry* **1993**, *4*, 1799–1802.

(42) Jurczak, J.; Pikul, S.; Bauer, T. *Tetrahedron* **1986**, *42*, 447.

(43) De Wilde, H.; De Clercq, P.; Vandewalle, M.; Röper, H. *Tetrahedron Lett.* **1987**, 4757, 4759.

(44) Coutts, S. J.; Kallmerten, J. *Tetrahedron Lett.* **1990**, *31*, 4305–4308.

(45) Nagase, S.; Uchibori, Y. *Tetrahedron Lett.* **1982**, *23*, 2585–2588.

(46) Nakamura, M.; Nakamura, E.; Koga, N.; Morokuma, K. *J. Chem. Soc., Faraday Trans.* **1994**, *90*, 1789–1798.

(47) Stewart, J. J. P. In *Reviews in computational chemistry*; Lipkowitz, K. B., Boyd, D. B., Eds.; VCH Publishers, Inc.: New York, 1990; pp 45–81.

(48) Zerner, M. C. In *Reviews in computational chemistry II*; Lipkowitz, K. B., Boyd, D. B., Eds.; VCH Publishers: New York, 1991; Vol. 2, pp 313–365.

(49) Stewart, J. J. P. *J. Comput. Chem.* **1989**, *10*, 209.

(50) Pietro, W. J.; Francl, M. M.; Hehre, W. J.; Defrees, D. F.; Pople, J. A.; Binkley, J. S. *J. Am. Chem. Soc.* **1982**, *104*, 5039.

(51) Frisch, M. J.; Trucks, G. W.; Head-Gordon, M.; Gill, P. M.; Wong, M. W.; Foresman, J. B.; Johnson, B. G.; Schlegel, H. B.; Robb, M. A.; Replogle, E. S.; Gomperts, R.; Andres, J. L.; Raghavachari, K.; Binkley, J. S.; Gonzalez, C.; Martin, R. L.; Fox, D. J.; Defrees, D. J.; Baker, J.; Stewart, J. J. P.; Pople, J. A. *GAUSSIAN92, Revision A*; Gaussian, Inc., Pittsburgh, PA, 1992.

(52) Schlegel, H. B. *J. Comput. Chem.* **1982**, *3*, 214.

(53) Schlegel, H. B. *J. Chem. Phys.* **1982**, *77*, 3676.

(54) Tsai, C. J.; Jordan, K. D. *J. Phys. Chem.* **1993**, *97*, 11227.

(55) McIver, J., Jr. *Acc. Chem. Res.* **1974**, *7*, 72.

(56) Fukui, K. *J. Phys. Chem.* **1970**, *74*, 4161.

(57) González, C.; Schlegel, H. B. *J. Phys. Chem.* **1990**, *94*, 5523.

(58) González, C.; Schlegel, H. B. *J. Chem. Phys.* **1991**, *95*, 5853.

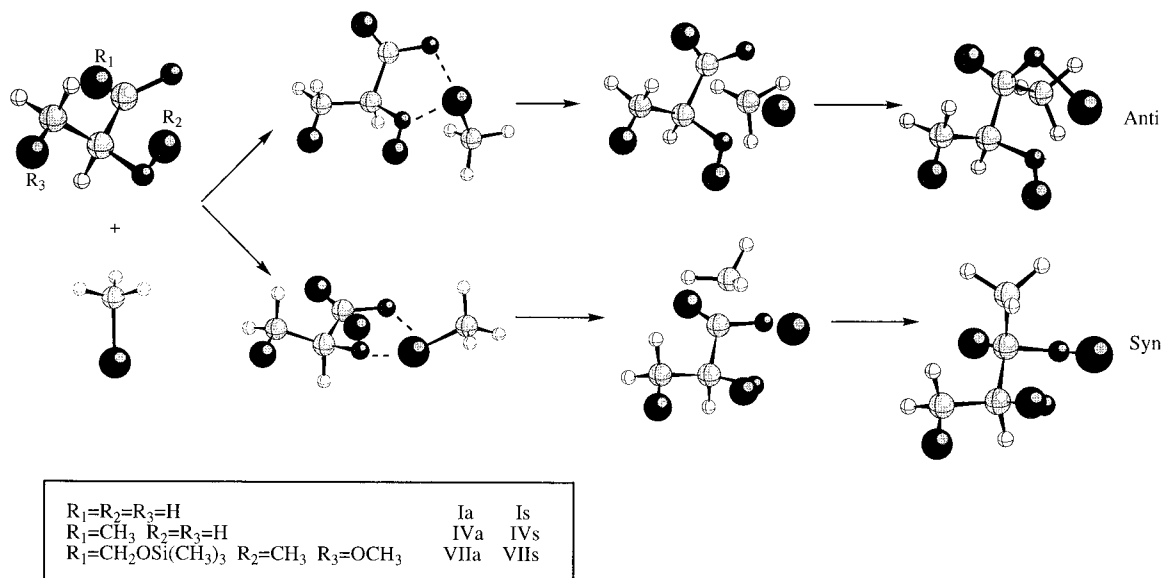
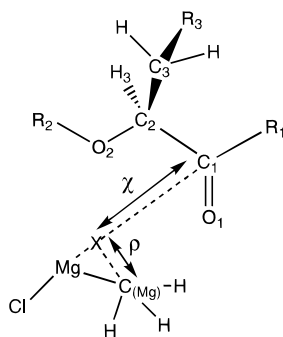


Figure 1. Reactants, chelate complexes, TSs, and products for the anti (upper path) and syn (lower path) addition of CH_3Mg^+ to **1** (Ia and Is processes, respectively), **2** (IVa and IVs processes), and **3** (VIIa and VIIs processes).

Chart 1. Definition of χ and ρ Variables Corresponding to the Main Components of the Transition Vector in the Case of a 1:1 Reaction^a

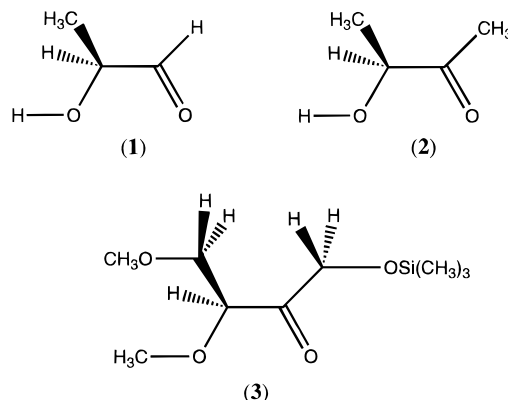


^a The numbering of the atoms is also shown. For the intermolecular reaction process, 1:2 reaction, Mg and $C_{(Mg)}$ correspond to the organomagnesium equivalent that carries out the addition process.

by us in calculating TSs, the atoms participating in the chemical interconversion are named as reactive space atoms and the related degrees of freedom belong to the control space of TV; those making the specificity of the substrates, bound outside the active space, are named nonreactive atoms, and the related degrees of freedom belong to the complementary space of TV.⁵⁹⁻⁶² A representation of the variables χ and ρ , which are included in the control space in the case of an intramolecular reaction mechanism, together with the numbering of the atoms directly involved in the chemical process, are depicted in Chart 1.

The use of appropriate minimal molecular models sustaining the actual chemical reaction is fundamental to generate reliable data. These systems must contain the intrinsic potentialities of the real system. In the present work two organomagnesium reagents have been selected: CH_3Mg^+ and CH_3MgCl . For the latter, the addition of 1 and 2 equiv to the substrate, which will correspond to an intramolecular and an intermolecular addition mechanism, respectively, has been

Chart 2. 2-Hydroxypropanal (1), 3-Hydroxybutanone (2), and 3,4-Di-*O*-methyl-1-*O*-(trimethylsilyl)-*L*-erythrulose (3), the Systems Considered Here as Models Representing the Real Substrate (3,4-Di-*O*-benzyl-1-*O*-*tert*-(Butyldiphenylsilyl)-*L*-erythrulose) Used by Us in the Reaction



studied. For representing the chiral α -alkoxy carbonyl compounds, three systems have been considered in the conformation shown in Chart 2: 2-hydroxypropanal (**1**), 3-hydroxybutanone (**2**) and 3,4-di-*O*-methyl-1-*O*-(trimethylsilyl)-*L*-erythrulose (**3**) The latter compound can be considered as a model representing the real substrate (3,4-di-*O*-benzyl-1-*O*-*tert*-butyldiphenylsilyl)-*L*-erythrulose) used by us⁴¹ in the reaction. The reactions studied here are the addition of CH_3Mg^+ , CH_3MgCl , and $2CH_3MgCl$ to the carbonyl group of **1**, **2**, and **3**. These models are somewhat simpler than the compounds used experimentally but likely embody the important features for this discussion. The additions of CH_3Mg^+ , CH_3MgCl , and $2CH_3MgCl$ to **1** and **2** have been studied by using PM3 and HF/3-21G theoretical methods; however, the large size of system **3** prevents its study at the *ab initio* level.

The reaction pathways and the stationary points characterized in this work are summarized in Figures 1-3.

Results and Discussion

1. Energetics. In order to discriminate between alternative reaction channels, a characterization of the PESs including the localization of stationary points is essential. An extensive exploration of the different PESs

(59) Tapia, O.; Andres, J. *Chem. Phys. Lett.* **1984**, *109*, 471-477.

(60) Andres, J.; Cárdenas, R.; Silla, E.; Tapia, O. *J. Am. Chem. Soc.* **1988**, *110*, 666-672.

(61) Tapia, O.; Andres, J.; Safont, V. S. *J. Chem. Soc., Faraday Trans.* **1994**, *90*, 2365-2374.

(62) Tapia, O.; Andres, J.; Safont, V. S. *J. Phys. Chem.* **1994**, *98*, 4821-4830.

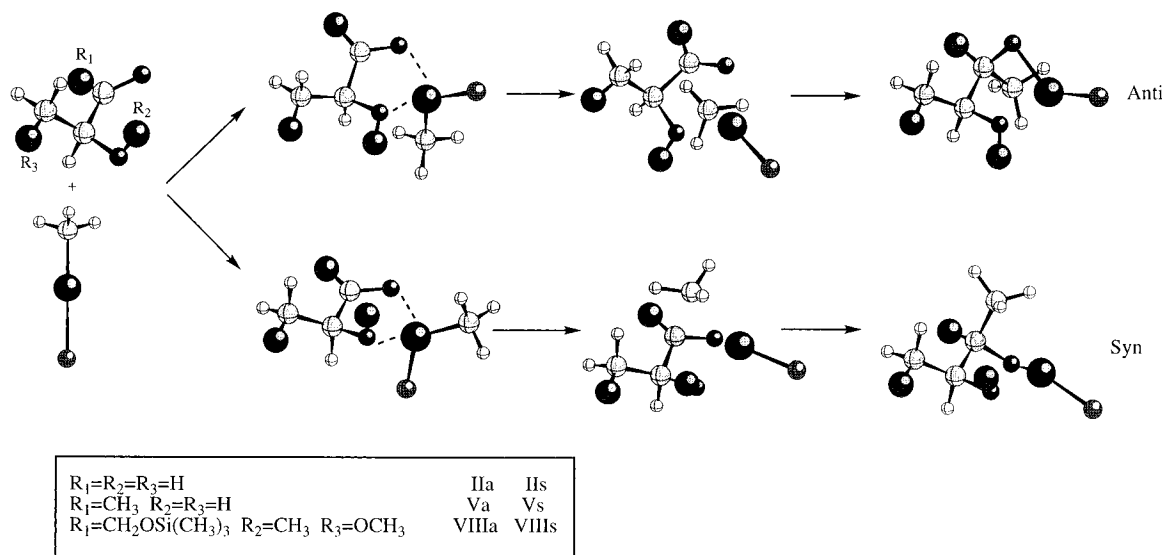


Figure 2. Reactants, chelate complexes, TSs, and products for the anti (upper path) and syn (lower path) addition of CH_3MgCl to **1** (IIa and IIs processes), **2** (Va and Vs processes), and **3** (VIIIa and VIIIs processes).

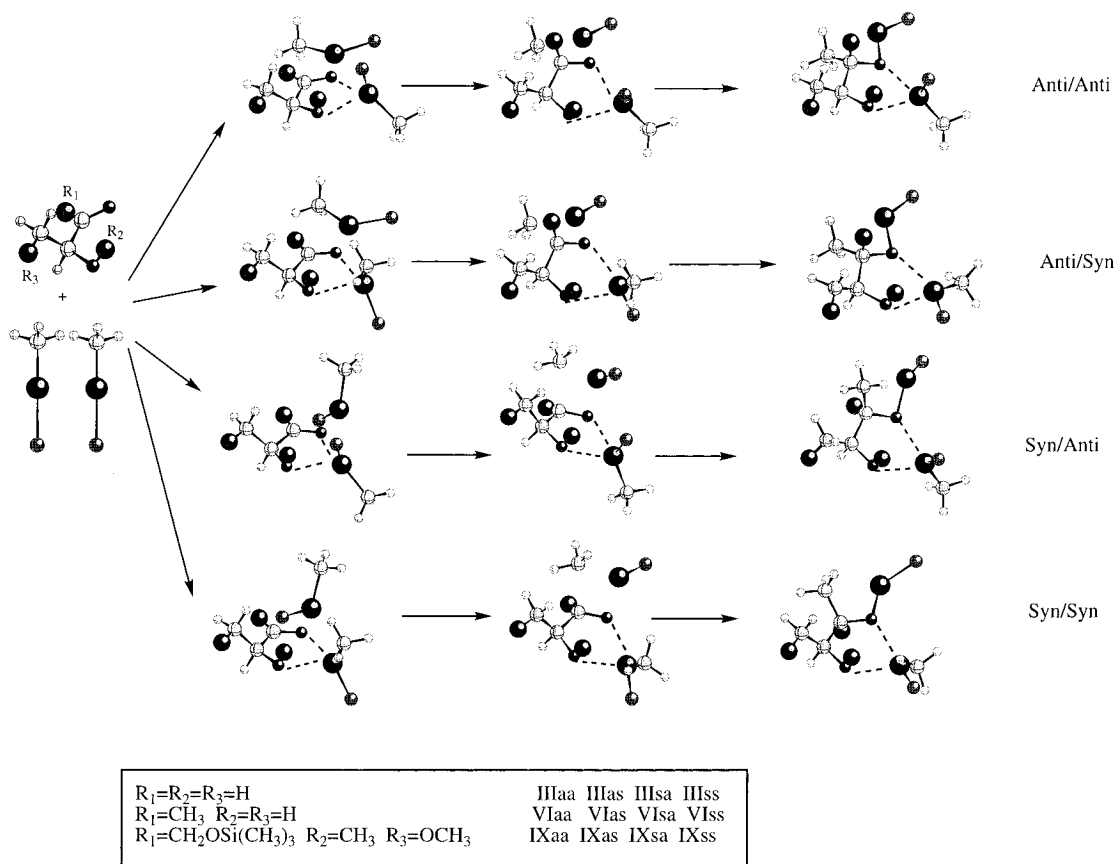


Figure 3. Reactants, chelate complexes, TSs, and products for the anti (two upper paths) and syn (two lower paths) addition of CH_3MgCl to **1** (IIIaa, IIIas, IIIsa, and IIIss processes), **2** (VIaa, VIas, VIsa, and VIss processes), and **3** (IXaa, IXas, IXsa, and IXss processes) with the participation of 2 equiv of CH_3MgCl . The relative orientation of the methyl group of the chelating CH_3MgCl can be anti (first and third paths) or syn (second and fourth paths) with respect to the CH_2R_3 group of the model.

has rendered two minima (chelate complexes and products) and one TS. In Table 1 we present the calculated energies of the chelate complexes, TSs, and products relative to reactants for the different reaction pathways. The following stationary points are found: the reactants, the chelate complexes (Ch) for the syn and anti attacks, the TS associated with 1,3-migration of the methyl group, and the corresponding products (P). The addition within

an intramolecular mechanism of the two organomagnesium compounds, CH_3Mg^+ and CH_3MgCl , to the molecular models **1**, **2**, and **3** gives rise to the **Ia**, **Is**, **IIa**, **IIs**, **IVa**, **IVs**, **Va**, **Vs**, **VIIa**, **VIIIs**, **VIIIa**, and **VIIIIs** processes (see Figures 1 and 2). For an intermolecular mechanism, corresponding to the participation of 2 equiv of CH_3MgCl , there are four competitive pathways: attack on anti and metal-chelated anti conformations (**IIIaa**, **VIaa**, and

Table 1. Relative Energies (kcal/mol) to Reactants of the Corresponding Chelates (Ch), Transition Structures (TS), and Products (P)^a

	PM3			HF/3-21G		
	Ch	TS (barrier height)	P	Ch	TS (barrier height)	P
Ia	-78.71	-35.34 (43.37)	-72.74 (5.97)	-100.79	-51.78 (49.01)	-96.23 (4.56)
Is	-78.76	-34.35 (44.41)	-75.03 (3.73)	-100.77	-50.11 (50.66)	-95.53 (5.24)
IIa	-48.45	-18.88 (29.57)	-60.56 (-12.11)	-52.77	-29.91 (22.86)	-85.26 (-32.49)
IIIs	-50.32	-18.15 (32.17)	-62.61 (-12.29)	-52.02	-28.13 (23.89)	-84.58 (-32.56)
IIIaa	-51.79	-28.65 (23.14)	-72.80 (-21.01)	-74.87	-65.09(9.78)	-145.75(-70.88)
IIIas	-49.12	-25.50 (23.62)	-70.61 (-21.49)	-77.71	-66.74 (10.97)	-149.92(-72.21)
IIIsa	-53.95	-27.45 (26.50)	-69.69 (-15.74)	-86.13	-75.01 (11.12)	-147.85 (-61.72)
IIIss	-51.50	-25.04 (26.46)	-67.89 (-16.39)	-89.44	-71.68 (17.76)	-148.34 (-58.90)
IVa	-79.51	-33.70 (45.81)	-67.79 (11.72)	-106.41	-53.22 (53.19)	-91.38 (15.03)
IVs	-79.71	-33.10 (46.61)	-70.74 (8.97)	-106.39	-50.46 (55.93)	-91.62 (14.77)
Va	-47.27	-15.58 (31.69)	-54.61 (-7.34)	-54.99	-29.70 (25.29)	-80.49 (-25.50)
Vs	-48.61	-14.57 (34.04)	-57.43 (-8.82)	-54.11	-26.67 (27.44)	-80.11 (-26.00)
VIaa	-49.41	-22.28 (27.13)	-67.84 (-18.43)	-80.95	-58.11 (22.84)	-140.31 (-59.36)
VIas	-46.33	-19.37 (26.96)	-65.70 (-19.37)	-83.65	-60.51 (23.14)	-139.43 (-55.78)
VIsa	-55.90	-22.16 (33.74)	-67.94 (-12.04)	-92.23	-68.85 (23.38)	-143.79 (-51.56)
VIss	-52.88	-20.44 (32.44)	-65.71 (-12.83)	-94.40	-61.85 (32.55)	-144.20 (-49.80)
VIIa	-87.79	-38.19 (49.60)	-74.62 (13.17)			
VIIIs	-85.31	-37.71 (47.60)	-76.13 (9.18)			
VIIIa	-49.76	-12.31 (37.45)	-55.42 (-5.66)			
VIIIIs	-47.24	-11.71 (35.53)	-57.70 (-10.46)			
IXaa	-41.83	-9.90 (31.93)	-54.79 (-12.96)			
IXas	-41.23	-8.75 (32.48)	-52.93 (-11.70)			
IXsa	-51.26	-13.06 (38.20)	-60.88 (-9.62)			
IXss	-50.28	-13.59 (36.69)	-59.50 (-9.22)			

^a Relative energies (kcal/mol) to Ch for TS (barrier height) and P in parentheses. For the PM3 results, heats of formation (hartrees) of the reactants are as follows: **I** = 0.169 146; **II** = -0.193 521; **III** = -0.243 680; **IV** = 0.154 497; **V** = -0.208 171; **VI** = -0.258 330; **VII** = -0.043 010; **VIII** = -0.405 678; **IX** = -0.455 837. For 3-21G results, total energies (hartrees) of the reactants are: **I** = -502.912 481; **II** = -960.562 903; **III** = -1655.814 261; **IV** = -541.745 449; **V** = -999.395 871; **VI** = -1694.647 229.

IXaa processes), attack on syn and metal-chelated anti conformations (**IIIsa**, **VIsa**, and **IXsa**), attack on anti and metal chelated syn conformations (**IIIas**, **VIas**, and **IXas**), and attack on syn and metal-chelated syn conformations (**IIIss**, **VIss**, and **IXss**) (see Figure 3).

The first step corresponds to the formation of a stable chelate complex without energy barrier. This result is in agreement with experimental work reported by Eliel et al.^{9,63} and Reetz et al.,⁶⁴ showing that the α -chelate is a true reaction intermediate. The second and rate-limiting step is the 1,3-migration of the CH₃ group of the nucleophile from the chelate complex via TS to products. It is important to note that the π -complex was not found as a stationary point on PES. The π -complexation step in the α -chelation process has been suggested by Corcoran and Ma.⁶⁵ Our results confirm that this step can be discarded, in agreement with related theoretical^{35,46} and experimental studies.⁶⁶⁻⁶⁹

For the addition of CH₃Mg⁺ to **1**, **Ia**, and **Is** processes, the chelate complexes are the most stable systems (79 and 100 kcal/mol below the reactants for PM3 and HF/3-21G methods, respectively) and the barrier heights are in the range 43–44 kcal/mol and 49–50 kcal/mol for PM3 and HF/3-21G, respectively. The product of the syn attack (**Is**) is more stable than the product of the anti attack (**Ia**) at semiempirical approach while an opposite result is found at the *ab initio* level. The addition of CH₃-

MgCl to the carbonyl group of **1**, **IIa**, and **IIIs** processes presents barrier heights of 30–32 kcal/mol (PM3) and 23–24 kcal/mol (HF/3-21G). In this case, the products are the most stable species (12 and 33 kcal/mol below the chelate complexes for PM3 and HF/3-21G methods, respectively). In these four cases, both methods render that the anti attack is the most favorable pathway. In the case of 2:1 stoichiometry (addition of 2 equiv of CH₃-MgCl to the carbonyl group of **1**; **IIIaa**, **IIIas**, **IIIsa**, and **IIIss** processes) the barrier heights are predicted to be lower than in the case of 1:1 stoichiometry (23–27 and 10–18 kcal/mol for PM3 and HF/3-21G methods, respectively). For the anti attack case (**IIIaa** and **IIIas** processes) the most favorable pathways are those with a lower energy barrier and a larger stability for the products than the syn attack (**IIIsa** and **IIIss** processes).

For the additions of CH₃Mg⁺, CH₃MgCl, and 2 equiv of CH₃MgCl to **2**, **IVa**, **IVs**, **Va**, **Vs**, **VIaa**, **VIas**, **VIsa**, and **VIss** processes, the barrier height increases for all cases with respect to the above results as shown in Table 1. It is important to note that subtle structural differences determine the barrier heights. Once the chelate is formed, the aldehyde reacts faster than the ketone. The stability of the chelate complexes is predicted to be 0.8–5.6 kcal/mol larger for this model than for the **1** chelate system at the *ab initio* level, likely reflecting the lower Lewis basicity of an aldehyde than that of a ketone. The aldehyde is more reactive because its lower basicity makes the complex less stable than the ketone. However, PM3 results do not show this trend, due to the poor description of noncovalent interactions.

The inclusion of protective groups on C₁, C₂, and O₃ centers in α -alkoxy ketones, which will correspond to the additions of CH₃Mg⁺, CH₃MgCl, and 2CH₃MgCl to **3** (**VIIa**, **VIIIs**, **VIIIa**, **VIIIIs**, **IXaa**, **IXas**, **IXsa**, and **IXss** processes), increases the barrier heights (1–6 kcal/mol) and decreases the products stability (0.2–3.6 kcal/mol)

(63) Frye, S. V.; Eliel, E. L.; Cloux, R. *J. Am. Chem. Soc.* **1987**, *109*, 1862–1863.

(64) Reetz, M. T.; Raguse, B.; Seitz, T. *Tetrahedron* **1993**, *49*, 8561–8568.

(65) Corcoran, R. C.; Ma, J. *J. Am. Chem. Soc.* **1992**, *114*, 4536.

(66) Poll, T.; Metter, J. O.; Helmchen, G. *Angew. Chem., Int. Ed. Engl.* **1985**, *24*, 112.

(67) Buhro, W. E.; Georgiou, S.; Fernández, J. M.; Patton, A. T.; Strouse, C. E.; Gladysz, J. A. *Organometallics* **1986**, *5*, 956.

(68) Shambayati, S.; Crowe, W. E.; Schreiber, S. L. *Angew. Chem., Int. Ed. Engl.* **1990**, *29*, 256.

(69) Arai, M.; T., K.; Nakamura, E. *J. Org. Chem.* **1993**, *58*, 5121.

Table 2. Calculated Product Ratio for the Diastereomers Obtained by Means of an Anti Attack of the Organomagnesium Reagent Methyl Group with Respect to Those Obtained by Means of a Syn Attack^a

	PM3	HF/3-21G
I	85:15	94:6
II	99:1	85:15
III	99:1	92:8
IV	79:21	99:1
V	98:2	97:3
VI	>99:1	85:15
VII	3:97	
VIII	4:96	
IX	>99:1	

^a The results obtained with the different model systems used are shown. The experimental product ratio,⁴¹ obtained with an excess of methylmagnesium chloride and 3,4-di-*O*-benzyl-1-*O*-(*tert*-butyldiphenylsilyl)-L-erythrulose, is >99:1.

with respect to the preceding cases. The calculated energetics indicate that the anti nucleophilic attacks, **IXaa** and **IXas** processes, present lower energy barriers and higher stabilities for the corresponding products than the syn attacks, **IXsa** and **IXss** processes.

The ratio between the product obtained by means of an anti attack with respect to that obtained by a syn attack can be calculated, assuming a Boltzmann's distribution of the TS leading to the two diastereomers, by using the following equation³²

$$\text{anti/syn} = \frac{\sum e^{-\Delta E_a/RT}}{\sum e^{-\Delta E_s/RT}} \quad (1)$$

where anti and syn refer to the TS conformation and ΔE_a and ΔE_s are the relative energies of the TSs for the anti and syn attack, respectively, with respect to the correspondent chelate complexes. In Table 2 we show the results obtained for the different processes studied here, together with the experimental ratio (>99:1, anti:syn) obtained by us.⁴¹ Although some differences can be detected when comparing the results obtained with semiempirical and *ab initio* methods, both offer the same trends and are in qualitatively good agreement with the experimental value. When using **3** as molecular model, we find that the product ratio is inverted with respect to the experimental result if an intramolecular mechanism (**VII** and **VIII** processes) is considered. However, if the mechanism is intermolecular (**IX**), the experimental product ratio is theoretically reproduced.

The possibility of an interconversion between the chelate complexes must be investigated. If this process takes place, then an equilibrium could be established between both chelate complexes, and according to the Curtin–Hammet principle, the product ratio would depend only on the relative energy of the two TSs. However, the estimated barriers for the interconversion between chelate complexes are higher than the corresponding barriers for addition and this fact would prevent such an equilibrium from being established.

Our results show that the anti attacks and the intermolecular mechanisms are energetically favorable, in agreement with the cyclic, or chelate, Cram model.^{14,15} According to this model, if a group on the adjacent chiral center is capable of chelation, *i.e.*, if it contains an oxygen or nitrogen moiety in the α - or β -position, the substituent containing the oxygen or nitrogen atom is held in an approximately coplanar arrangement by simultaneous chelation with the metal counterion and the nucleophile attacks from the least hindered face. This model is

especially operative in the case of α -alkoxy and α -hydroxy carbonyl compounds.

2. Structure. The selected geometrical parameters for the different model systems are supplied as supporting information. The completely optimized geometries are available from the authors upon request. An analysis of the results reveals slight differences depending on the computational level and model system used, but similar geometric variables have been found.

The chelate structures are puckered five-membered rings; the metal is coordinated to the lone pair of the carbonyl oxygen, and the methoxy oxygen is not pyramidalized. Similar structures have been found for related chelates using the X-ray method⁷⁰ and related theoretical calculations.^{35,46,71} There is a correlation between reactivity and stereoselectivity that demonstrates the mechanistic importance of chelation, as the chelate structure is maintained throughout the reaction path.

The intramolecular conversion of the chelate complex to the product takes place via the corresponding TS with retention of the chelate configuration. For CH_3Mg^+ and CH_3MgCl systems, the nucleophilic methyl group of the organomagnesium compound is located over or above the chelate ring at TS structure. The steric interactions with the α -substituted group, CH_2R_3 , are avoided in the cases of anti attack, which is consistently favored. On the other hand, the steric interactions between the nucleophilic methyl group and the R_1 group increase with the size of R_1 : an aldehyde hydrogen in **1**, a methyl group in **2**, and a [(trimethylsilyl)oxy]methyl group in **3**. This fact can explain the difference of barrier heights, from the chelate complex to the TS, increasing in the order 2-hydroxypropanal < 3-hydroxybutanone < 3,4-di-*O*-methyl-1-*O*-(trimethylsilyl)-L-erythrulose for both PM3 and HF/3-21G methods.

The inclusion of a CH_3MgCl second molecule lends support to an assisted intermolecular mechanism, where the first molecule forms the chelate structure and the second CH_3MgCl molecule carries out the nucleophilic addition to the carbonyl group. This fact is in agreement with experimental data reported by Reetz et al.⁶⁴

3. Bond Orders. In order to calculate the progress of the chemical processes, Pauling bond orders⁷² (BO) were calculated for TSs, chelate complexes, and products through the following expression

$$\text{BO} = \exp[|R(1) - R(\text{TS})|/0.3] \quad (2)$$

where $R(\text{TS})$ represents the length corresponding to a bond in the TS, chelate complex, or product and $R(1)$ represents the reference bond length. For the breaking bond ($\text{Mg}-\text{C}_{(\text{Mg})}$), the bond order at chelate complexes was set to 1 by using as $R(1)$ the equilibrium distances in chelate complex; analogously, for the forming bond ($\text{C}_{(\text{Mg})}-\text{C}_1$), the bond order at products was set to one by using as $R(1)$ the equilibrium length in products and for the C_1-O_1 bond, which evolves from double to single, the bond order at products was set to one by using as $R(1)$ the equilibrium length of the single bond in products. The progress of the chemical process at TS was then evalu-

(70) Reetz, M. T.; Harms, K.; Reif, W. *Tetrahedron Lett.* **1988**, 29, 5881–5884.

(71) Jonas, V.; Frenking, G.; Reetz, M. T. *Organometallics* **1993**, 12, 2111.

(72) Pauling, L. *J. Am. Chem. Soc.* **1947**, 69, 542.

Table 3. Percentages of Evolution of the Reaction at TSs, Calculated through Eq 3, for the Forming Bond $C_{(Mg)}-C_1$, the Breaking Bond, $Mg-C_{(Mg)}$, and the C_1-O_1 Bond, which Evolves from Double to Single

	PM3			HF/3-21G		
	$C_{(Mg)}-C_1$	$Mg-C_{(Mg)}$	C_1-O_1	$C_{(Mg)}-C_1$	$Mg-C_{(Mg)}$	C_1-O_1
Ia	10.84	79.97	39.19	9.25	31.52	41.61
Is	10.72	80.10	40.06	8.57	28.36	41.73
IIa	6.49	81.38	24.51	5.53	31.66	26.12
IIs	6.32	81.84	24.77	5.25	29.56	26.35
IIIaa	11.35	38.37	41.09	3.61	15.53	23.12
IIIas	11.04	36.80	40.00	4.61	21.37	31.01
IIIsa	11.78	47.65	41.45	2.70	24.15	14.86
IIIss	11.60	49.33	40.74	2.38	25.55	5.67
IVa	11.21	82.68	41.82	10.47	32.16	47.63
IVs	10.23	81.58	41.36	9.83	29.14	47.82
Va	6.82	83.37	26.27	6.72	33.21	33.30
Vs	5.97	83.10	24.51	5.95	30.51	32.71
VIaa	6.57	80.49	29.60	4.92	19.69	35.51
VIas	6.34	79.51	28.96	3.76	12.69	33.18
VIsa	6.37	81.27	30.11	1.71	9.97	11.36
VIss	6.42	81.88	30.11	4.64	29.61	28.86
VIIa	12.38	84.81	42.35			
VIIs	10.45	82.74	39.02			
VIIIa	7.45	85.56	26.37			
VIIIs	6.14	84.02	23.60			
IXaa	10.94	37.16	46.04			
IXas	11.07	35.68	43.79			
IXsa	6.84	80.47	31.38			
IXss	7.04	81.14	31.38			

ated for each one of these three bonds through the following expression

$$\% \text{ evolution} = \frac{\text{BO}(\text{TS}) - \text{BO}(\text{Ch})}{\text{BO}(\text{P}) - \text{BO}(\text{Ch})} \times 100 \quad (3)$$

where BO(TS), BO(Ch), and BO(P) represent the calculated bond orders for TS, chelate complexes, and products, respectively. Calculated percentages of evolution at TSs are reported in Table 3.

A detailed analysis of these data shows that the methodology employed has a great influence on the results obtained. PM3 results show that in the TS the $C_{(Mg)}-C_1$ bond formation is in the range of 6–12% evolution, while for the $Mg-C_{(Mg)}$ bond breaking the range is very wide (35–85%), depending on the molecular mechanism and the size of the molecular model used. A comparison of PM3 data with *ab initio* results show a similar degree of formation for the $C_{(Mg)}-C_1$ bond (2–10%) but a lower percentage of breaking for the $Mg-C_{(Mg)}$ bond (10–33%). The evolution of the C_1-O_1 bond at TS is smaller than 50%: PM3 results indicate a range between 23.60 and 46.04%, while for HF/3-21G the range is 5.67–47.82%.

For the intramolecular mechanism of addition, both in the PM3 and the *ab initio* methods, the influence on these results of the relative orientation at the TS between the methyl group of organomagnesium reagent and the α -carbon methyl group of the substrate (anti or syn attacks) is hardly pronounced (less than 3% in all cases). However, for the intermolecular mechanism, significant differences have been detected. For example, at the PM3 level, **IXaa** and **IXas** processes show a 35–37% of $Mg-C_{(Mg)}$ bond breaking, while **IXsa** and **IXss** processes render 80–81%.

With respect to the organomagnesium reagent, for the intramolecular mechanism the degree of forming and breaking bonds is roughly independent of the model representing the substrate. However, in the case of an intermolecular mechanism, differences can be detected;

Table 4. Hessian Unique Negative Eigenvalue (au), Imaginary Frequency (cm^{-1}) Obtained from a Normal Mode Analysis, Force Constants (F , au), and Hessian Eigenvector Components (C) for the TS. Addition of CH_3Mg^+ to 2-Hydroxypropanal, 1

Eig freq	PM3				HF/3-21G			
	Ia		Is		Ia		Is	
	F	C	F	C	F	C	F	C
C_1-O_1	0.59	0.15	0.59	0.13	0.48	0.17	0.48	0.11
χ	0.00	-0.84	0.00	-0.86	0.01	-0.73	0.02	-0.80
ρ	0.10	-0.19	0.10	-0.11	0.11	-0.30	0.11	-0.29
$O_1-C_1-C_2$	4.64	-0.07	4.64	-0.04	1.10	-0.06	1.13	-0.08
$O_1-C_1-C_2-O_2$	0.69	-0.10	0.43	0.11	0.56	-0.15	0.53	0.17

Table 5. Hessian Unique Negative Eigenvalue (au), Imaginary Frequency (cm^{-1}) Obtained from a Normal Mode Analysis, Force Constants (F , au), and Hessian Eigenvector Components (C) for the TS. Addition of CH_3MgCl to 2-Hydroxypropanal, 1

Eig freq	PM3				HF/3-21G			
	Ia		Is		Ia		Is	
	F	C	F	C	F	C	F	C
C_1-O_1	0.72	0.11	0.72	0.10	0.63	0.10	0.63	0.10
χ	0.01	-0.84	0.01	-0.83	0.01	-0.76	0.01	-0.75
ρ	0.10	-0.20	0.10	-0.18	0.09	-0.17	0.09	-0.28
$O_1-C_1-C_2$	4.53	-0.09	4.65	-0.00	0.99	-0.18	1.03	-0.14
$O_1-C_1-C_2-O_2$	0.78	-0.10	0.46	0.10	0.55	-0.14	0.52	0.03

for instance, at PM3 results, a significant increase of $Mg-C_{(Mg)}$ bond breaking appears from **III** (37–49%) to **VI** (79–82%).

In the intramolecular mechanism, the CH_3MgCl organomagnesium reagent retards the progress of the formation of the $C_{(Mg)}-C_1$ bond and the evolution of the C_1-O_1 bond with respect to CH_3Mg^+ and increases the progress of the breaking of $Mg-C_{(Mg)}$ bond.

4. Transition Vector. The TV renders very concisely the essentials of the chemical process under study. The corresponding TV as well as force constants for the variables defining the control space, imaginary frequency, and the unique negative eigenvalue are reported in Tables 4–12. The TSs are well associated with the forming/breaking bonds as can be seen from the main components of the TVs as well as going down from the TS following the reaction path by using the IRC procedure. The results provide good hints for a qualitative and semiquantitative analysis.

The normal mode analysis of TS structures yields a relatively low imaginary frequency ($468i$ – $707i \text{ cm}^{-1}$, for PM3 results and $111i$ – $570i \text{ cm}^{-1}$, for HF/3-21G results). For all model systems, the negative eigenvalue arises from the cross terms in the force constant matrix; diagonal force constants are all positive, and the values for force constants associated to χ and ρ are positive and very low. An analysis of the TV shows that the major components are χ and ρ distances and the $O_1-C_1-C_2-O_2$ dihedral angle. The minimal set of coordinates capable of producing the TS are these variables. This result is obtained after reducing the size of the control space followed by the diagonalization of the corresponding Hessian matrix.

It is important to note that while the atoms participating in the TSs are always the same, those entering in the complementary space are not. If these latter do not modulate in the first order the force constants in the

Table 6. Hessian Unique Negative Eigenvalue (au), Imaginary Frequency (cm⁻¹) Obtained from a Normal Mode Analysis, Force Constants (F, au), and Hessian Eigenvector Components (C) for the TS. Addition of 2CH₃MgCl to 2-Hydroxypropanal, 1

Eig freq	PM3								HF/3-21G							
	IIIaa		IIIas		IIIsa		IIIss		IIIaa		IIIas		IIIsa		IIIss	
	-0.102 47		-0.096 91		-0.106 23		I-0.032 93		-0.007 06		-0.041 98		-0.049 82		-0.011 60	
	518.30 <i>i</i>		513.85 <i>i</i>		565.02 <i>i</i>		564.91 <i>i</i>		306.75 <i>i</i>		385.03 <i>i</i>		286.93 <i>i</i>		275.40 <i>i</i>	
	F	C	F	C	F	C	F	C	F	C	F	C	F	C	F	C
C ₁ -O ₁	0.84	0.16	0.85	0.16	0.82	0.13	0.80	0.10	0.75	0.07	0.70	0.13	0.79	0.11	0.80	0.06
C ₁ -C _(Mg)	0.08	-0.65	0.08	-0.67	0.08	-0.68	0.08	-0.49	0.05	-0.64	0.05	-0.68	0.05	-0.70	0.04	-0.74
O ₁ -Mg	0.49	-0.11	0.48	-0.11	0.51	-0.07	0.51	-0.07	0.06	-0.13	0.06	-0.29	0.05	-0.08	0.06	-0.23
O ₁ -C ₁ -C ₂	4.06	-0.05	4.09	-0.05	4.81	-0.07	4.44	-0.01	1.93	-0.03	1.82	-0.02	2.05	-0.04	2.00	-0.04
O ₁ -C ₁ -C ₂ -O ₂	0.73	-0.07	0.75	-0.07	0.71	0.12	0.72	0.23	0.57	-0.16	0.71	-0.03	1.42	0.07	1.56	0.22

Table 7. Hessian Unique Negative Eigenvalue (au), Imaginary Frequency (cm⁻¹) Obtained From a Normal Mode Analysis, Force Constants (F, au), and Hessian Eigenvector Components (C) for the TS. Addition of CH₃Mg⁺ to 3-Hydroxybutanone, 2

Eig freq	PM3				HF/3-21G			
	IVa		IVs		IVa		IVs	
	-0.100 52		-0.079 76		-0.073 44		-0.023 76	
	680.78 <i>i</i>		671.40 <i>i</i>		570.89 <i>i</i>		569.03 <i>i</i>	
	F	C	F	C	F	C	F	C
C ₁ -O ₁	0.56	0.13	0.56	0.15	0.45	0.15	0.44	0.09
χ	0.01	-0.85	0.00	-0.85	0.02	-0.74	0.02	-0.82
ρ	0.12	-0.26	0.12	-0.20	0.11	-0.29	0.10	-0.31
O ₁ -C ₁ -C ₂	5.07	-0.05	5.20	-0.07	1.22	-0.09	1.26	-0.04
O ₁ -C ₁ -C ₂ -O ₂	0.65	-0.13	0.44	0.12	0.55	-0.18	0.53	0.15

Table 8. Hessian Unique Negative Eigenvalue (au), Imaginary Frequency (cm⁻¹) Obtained from a Normal Mode Analysis, Force Constants (F, au) and Hessian Eigenvector Components (C) for the TS. Addition of CH₃MgCl to 3-Hydroxybutanone, 2

Eig freq	PM3				HF/3-21G			
	Va		Vs		Va		Vs	
	-0.042 95		-0.039 68		-0.054 20		-0.088 93	
	523.59 <i>i</i>		499.38 <i>i</i>		428.24 <i>i</i>		434.36 <i>i</i>	
	F	C	F	C	F	C	F	C
C ₁ -O ₁	0.69	0.12	0.69	0.11	0.57	0.10	0.57	0.11
χ	0.01	-0.83	0.01	-0.83	0.02	-0.73	0.02	-0.79
ρ	0.12	-0.24	0.11	-0.26	0.09	-0.22	0.09	-0.16
O ₁ -C ₁ -C ₂	4.89	-0.06	5.13	-0.06	1.09	-0.10	1.14	-0.05
O ₁ -C ₁ -C ₂ -O ₂	0.76	-0.17	0.46	0.08	0.56	-0.08	0.51	0.16

control space, the TV is invariant. The invariance is to be understood in terms of preservation of the reactive fluctuation patterns associated with the chemical interconversion processes. In this respect, the TS presents similar geometric properties for the different model systems. One of the interesting results obtained is a sort of geometric invariance of the fragments participating in a TS geometry. This fact has been found by us^{61,62,73} and other workers.⁷⁴ Structural invariance of the TS structure fragments is an important result from the

technical viewpoint. It aids the establishment of the search of TSs.

Conclusions

Quantum chemical characterization of TSs may be rationalized to discuss the nature of molecular mechanism for organic reactions. The theory of nucleophilic addition of organometallic reagents to carbonyl compounds is still a much debated subject, particularly with respect to the origin of stereoselectivity. The following factors are found to be dominant in the molecular mechanism for the carbonyl addition of organomagnesium reagents to chiral α-alkoxy carbonyl compounds:

(i) The formation of syn and anti chelate complexes is the first step in the addition process and takes place without energy barrier. The magnesium is coordinated to the lone pair of the carbonyl oxygen and to the methoxy oxygen. The chelate complexes can be described as puckered five-membered rings.

(ii) Syn and anti chelate intermediates are stable structures, restricting bond rotation and increasing stereochemistry. The aldehyde chelate is less stable than the ketone chelates.

(iii) The chelate conformation is maintained throughout the reaction path, being the thermodynamic controls for the syn and anti pathway dominated by the relative stability between the corresponding chelate complexes and products. Cram's model based on chelation-controlled carbonyl addition can explain the energetic results.

(iv) C-C bond-forming stage is the second and rate-limiting step for the addition process. TSs are four-membered rings, corresponding to the 1,3-intramolecular migration from chelate complex to products.

(iv) The reactivity for chiral α-alkoxy carbonyl compounds decreases in the following order: 2-hydroxypropanal > 3-hydroxybutanone > 3,4-di-*O*-methyl-1-*O*-(trimethylsilyl)-*L*-erythrulose. Nevertheless, the increasing of the model size results in an increase of the barrier

Table 9. Hessian Unique Negative Eigenvalue (au), Imaginary Frequency (cm⁻¹) Obtained from a Normal Mode Analysis, Force Constants (F, au), and Hessian Eigenvector Components (C) for the TS. Addition of 2CH₃MgCl to 3-Hydroxybutanone, 2

Eig freq	PM3								HF/3-21G							
	VIaa		VIas		VIsa		VIss		VIaa		VIas		VIsa		VIss	
	-0.08267		-0.08756		-0.50363		-0.09818		-0.04843		-0.02069		-0.01404		-0.03698	
	550.83 <i>i</i>		546.80 <i>i</i>		568.69 <i>i</i>		570.41 <i>i</i>		422.79 <i>i</i>		388.22 <i>i</i>		111.64 <i>i</i>		430.49 <i>i</i>	
	F	C	F	C	F	C	F	C	F	C	F	C	F	C	F	C
C ₁ -O ₁	0.96	0.16	0.96	0.16	0.97	0.04	0.97	0.16	0.65	0.12	0.66	0.11	0.81	0.06	0.66	0.12
C ₁ -C _(Mg)	0.07	-0.69	0.07	-0.66	0.06	-0.49	0.06	-0.70	0.05	-0.82	0.05	-0.73	0.05	-0.78	0.05	-0.85
O ₁ -Mg	0.45	-0.10	0.45	-0.10	0.48	-0.11	0.47	-0.08	0.10	-0.36	0.07	-0.30	0.03	-0.47	0.08	-0.20
O ₁ -C ₁ -C ₂	5.69	-0.02	5.84	-0.02	5.70	-0.16	5.49	-0.05	1.75	-0.06	1.79	-0.07	1.88	-0.01	1.70	-0.04
O ₁ -C ₁ -C ₂ -O ₂	0.91	-0.05	0.94	-0.06	0.92	0.06	0.94	0.10	0.89	-0.04	0.94	-0.15	2.56	0.15	1.82	0.14

Table 10. Hessian Unique Negative Eigenvalue (au), Imaginary Frequency (cm⁻¹) Obtained from a Normal Mode Analysis, Force Constants (F, au), and Hessian Eigenvector Components (C) for the TS. Addition of CH₃Mg⁺ to 3,4-Di-*O*-methyl-1-*O*-(trimethylsilyl)-L-erythrose, 3

Eig freq	PM3			
	VIIa		VIIs	
	-0.07966 707.14i		-0.10487 694.26i	
	F	C	F	C
C ₁ -O ₁	0.55	0.17	0.56	0.17
χ	0.02	-0.79	0.02	-0.80
ρ	0.14	-0.30	0.12	-0.23
O ₁ -C ₁ -C ₂	6.89	-0.08	6.72	-0.10
O ₁ -C ₁ -C ₂ -O ₂	1.13	-0.08	1.23	0.09

Table 11. Hessian Unique Negative Eigenvalue (au), Imaginary Frequency (cm⁻¹) Obtained from a Normal Mode Analysis, Force Constants (F, au), and Hessian Eigenvector Components (C) for the TS. Addition of CH₃MgCl to 3,4-Di-*O*-methyl-1-*O*-(trimethylsilyl)-L-erythrose, 3

Eig freq	PM3			
	VIIIa		VIIIs	
	-0.052 47 550.66i		-0.047 02 535.84i	
	F	C	F	C
C ₁ -O ₁	0.68	0.10	0.70	0.11
χ	0.02	-0.83	0.02	-0.80
ρ	0.14	-0.24	0.12	-0.23
O ₁ -C ₁ -C ₂	7.05	-0.01	6.98	-0.08
O ₁ -C ₁ -C ₂ -O ₂	1.16	-0.08	1.21	0.15

Table 12. Hessian Unique Negative Eigenvalue (au), Imaginary Frequency (cm⁻¹) Obtained from a Normal Mode Analysis, Force Constants (F, au), and Hessian Eigenvector Components (C) for the TS. Addition of 2CH₃MgCl to 3,4-Di-*O*-methyl-1-*O*-(trimethylsilyl)-L-erythrose, 3

Eig freq	PM3							
	IXa		IXs		IXa		IXs	
	-0.108 31 536.31i		-0.094 32 531.73i		-0.395 42 573.65i		-0.111 19 570.96i	
	F	C	F	C	F	C	F	C
C ₁ -O ₁	0.91	0.16	0.91	0.16	1.01	0.18	1.01	0.17
C ₁ -C _(Mg)	0.07	-0.63	0.07	-0.66	0.05	-0.53	0.05	-0.70
O ₁ -Mg	0.50	-0.19	0.50	-0.10	0.51	-0.10	0.50	-0.08
O ₁ -C ₁ -C ₂	7.07	-0.03	7.13	-0.04	9.23	-0.13	9.13	-0.06
O ₁ -C ₁ -C ₂ -O ₂	3.95	-0.05	3.93	0.03	2.94	-0.11	2.93	0.06

height. The size of the substituent on C₁ is the dominant factor in the relative energy barriers, but not with respect to the stereoselectivity control.

(v) For the nature of the Grignard reagent, the barrier heights are lower for CH₃MgCl than for the cationic species, CH₃Mg⁺. The inclusion of a second CH₃MgCl

second molecule diminishes the barrier height, and the process can be described as an assisted intermolecular mechanism: the first molecule forms the chelate structure and the second CH₃MgCl molecule carries out the nucleophilic addition to carbonyl group. The chelate formation is fast, being the rate-limiting step the addition of the second CH₃MgCl molecule to the chelate complex, in agreement with the experimentally determined first-order kinetics in organometallic.⁹ The most favorable pathway corresponds to an anti attack via an intermolecular assisted mechanism. These theoretical results are in agreement with experimental data of Reetz et al.⁶⁴ and with the diastereoisomeric excess obtained by us.⁴¹

(vi) There are differences in absolute values for barrier height between the chelate complex and the corresponding TS and the relative stability of the products obtained with PM3 semiempirical and *ab initio* methods. However, the tendencies are similar.

(vii) The geometry and TV for TSs are fairly invariant. PM3 semiempirical results are very close to those of HF/3-21G. This is good news for increasing the size of the model.

(viii) There exists a minimal molecular model with a TS which describes the essentials of the chemical interconversion step in a given molecular mechanism and the corresponding TV that encodes the fundamental information relating reactive fluctuations patterns and is an invariant feature. Theoretical calculations of these type of stationary points on PES permit the actual determination of geometric structures and corresponding force constants.

Acknowledgment. This work was supported by research funds of the Ministerio de Educación y Ciencia, DGICYT (Project PB93-0661). Calculations were performed on an IBM RS6000 workstation of the Departament de Ciències Experimentals and on the cluster of Hewlett-Packard 9000/730 workstations of the Servei d'Informàtica of the Universitat Jaume I. We are indebted to these centers for providing us with computer capabilities. M.O. thanks the Ministerio de Educación y Ciencia for a FPI fellowship. R.C. thanks IBM for a fellowship.

Supporting Information Available: Tables 1s–5s (11 pages). This material is contained in libraries on microfiche, immediately follows this article in the microfilm version of the journal, and can be ordered from the ACS; see any current masthead page for ordering information.

JO952197X

(73) Andres, J.; Moliner, V.; Krechl, J.; Domingo, J. L.; Picher, M. T. *J. Am. Chem. Soc.* **1995**, *117*, 8807–8815.

(74) Ylioniemi, A.; Konschinn, H.; Neagu, C.; Pajunen, A.; Hase, T.; Brunow, G.; Teleman, O. *J. Am. Chem. Soc.* **1995**, *117*, 5120–5126.